

Resonant Raman scattering in a quasi-one-dimensional ZrS_3 crystal

Shalini Mathur, K. P. Jain, and R. K. Soni

Laser Technology Research Programme, Indian Institute of Technology, New Delhi 110 016, India

C. Julien and M. Balkanski

Laboratoire de Physique des Solides, Universite Pierre et Marie Curie, 4 place Jussieu, 75230 Paris CEDEX 05, France

(Received 12 February 1990; revised manuscript received 15 August 1990)

A theory of Raman scattering in one-dimensional crystals is presented, emphasizing resonance enhancement at the M_0 and M_3 singularities. A Slater-Koster model is used to incorporate the effect of electron-hole interaction. This leads to metamorphism of the critical points. Our experimental results show an enhancement of the one-phonon Raman intensity in a quasi-one-dimensional ZrS_3 crystal near the lowest-energy gap. They agree well with the theory both above and below the energy gap after including electron-hole interaction.

I. INTRODUCTION

The crystal structure of transition-metal trichalcogenides (MX_3) has been the subject of considerable interest for over a decade.¹⁻⁵ A large number of experimental studies have established a significant one-dimensional anisotropic character in these crystals.¹⁻¹¹ They¹² grow as fibrous ribbons with linear chain of metal atoms ($M=\text{Zr, Ti, Hf; Nb, Ta}$) parallel to the b crystallographic axis. Six chalcogen atoms ($X=\text{S, Se, Te}$) surround each metal atom forming a trigonal prism. The distance between metal atoms along the b axis is much shorter than the interprism distances. These structures^{13,14} have a bundle of metallic chains each with an insulating sheath. The interaction between chains is rather weak and therefore one-dimensional electronic behavior is expected from the structure. Similar stacking arrangement in NbSe_3 leads to high electrical conductivity along the linear chain direction.¹⁵ The conductivity perpendicular to the chains is, however, several hundred times smaller. Similar anisotropy is expected for TiS_3 (Ref. 16) and ZrS_3 also. High conductivity along the chain clearly indicates that the motion of electrons is restricted to one dimension, and that the material behaves as a quasi-one-dimensional crystal in its electronic properties.

The direct and indirect band gaps in ZrS_3 have been determined by optical-absorption spectra.¹⁷ From these optical studies it was concluded that the optical properties reflect the anisotropy of the crystal so that the band-gap energy of ZrS_3 is (2.56 ± 0.01) eV with an exciton ionization energy of (0.08 ± 0.01) eV for $\mathbf{E} \parallel \mathbf{b}$ and (2.57 ± 0.01) eV with an exciton ionization energy of (0.12 ± 0.01) eV for $\mathbf{E} \perp \mathbf{b}$. ZrS_3 shows a strong polarization dependence which indicates⁷ a large anisotropy in the band structure. Assuming a linear variation of band gap with temperature, we estimate that the band gap at 180 K is 2.54 eV. The M_0 and M_3 Van Hove singularities determine the optical properties of the quasi-one-dimensional systems. Consequently we identify the M_0 singularity at 2.54 eV.

The vibrational properties of ZrS_3 have been extensive-

ly studied^{2,7,18} by infrared and Raman spectroscopy. Infrared measurements revealed that the vibrations of the ZrS_3 crystal, both parallel and perpendicular to the chain axis, are one dimensional.⁶ Raman investigations²⁻⁵ exhibit a large number of phonons at the zone center which are characterized as A_g and B_g modes of C_{2h} crystal symmetry.

Resonant Raman scattering (RRS) in ZrS_3 near the lowest-energy gap transition has also been reported.^{7,18} Sourisseau and Mathey⁷ studied the interchain A_g modes and showed that strong enhancement in intensities of these modes can be accounted for by a Franck-Condon scattering mechanism. Kurita *et al.* argued¹⁸ that the intermediate state in the Raman process is $1S$ exciton. However, these authors have not calculated the exciton energy and have also not considered the effect of dimensionality on band-gap singularity which would be reflected in a resonant Raman experiment.

In this paper, we present a theory of resonant Raman scattering at the M_0 and M_3 critical points of a one-dimensional semiconductor for free electron-hole pairs as intermediate scattering states. It was assumed in the theory that the various components of the scattering matrix elements of the Raman tensor were basically independent of the photon energies and were assumed to be constants. These constant matrix elements correspond to averaging over the different components of the Raman tensor. The effect of electron-hole interaction on scattering is discussed by using the Slater-Koster interaction. Electron-hole interaction leads to metamorphism of the singularities. We also present experimental results on resonant Raman scattering on one-dimensional ZrS_3 near the energy gap transition. We have conducted Raman experiments for the M_0 critical point stressing the resonant nature of the scattering process. For experiment, the scattering photons were detected unanalyzed corresponding to averaging over the anisotropies. The one-phonon A_g modes show enhancement at the energy gap. Our experimental results agree well with the theory both below and above the energy gap after including electron-hole interaction.

II. THEORY OF RAMAN SCATTERING NEAR THE SINGULARITIES: NO ELECTRON-HOLE INTERACTION

Consider Raman scattering (RS) in one-dimensional crystals near the Van Hove singularities assuming free electron-hole pairs as intermediate scattering states. The one-phonon RS amplitude¹⁹ at the M_0 edge is then given by

$$A(\omega) \sim \int_0^{k_{\max}} \frac{dk_z}{[\omega_g - \omega + \omega_0 + (hk_z^2/2m) + i\Gamma][\omega_g - \omega + (hk_z^2/2m) + i\Gamma]}, \quad (1)$$

where ω and ω_0 are the energies of the incident photon and phonon, respectively. The momentum dependence of scattering matrix elements has been neglected in Eq. (1), Γ being the damping factor associated with lifetimes of the intermediate scattering states. Since not much is known about the nature of the relaxation processes in ZrS_3 , we prefer to treat the phenomenological parameter Γ as a constant.

Assuming parabolic bands,

$$\omega_k = \omega_g + hk_z^2/2m, \quad (2)$$

where k_z is the total wave vector and ω_g is the band gap. Then, Eq. (1) becomes

$$A(\omega) \sim \int_{\omega_g}^{\infty} \frac{d\omega_k (\omega_k - \omega_g)^{-1/2}}{(\omega_k - \omega + i\Gamma)(\omega_k - \omega + \omega_0 + i\Gamma)}. \quad (3)$$

Extending the upper limit to k by taking $k_{\max} = \infty$, this integral can be evaluated with the contour given in Fig. 1. The Raman amplitude at the M_0 edge is

$$A(\omega) \sim \frac{1}{\omega_0} \left[\frac{\sin\theta_1}{[(\omega - \omega_g)^2 + \Gamma^2]^{1/2}} - \frac{\sin\theta_2}{[(\omega - \omega_0 - \omega_g)^2 + \Gamma^2]^{1/4}} \right] + \frac{i}{\omega_0} \left[\frac{\cos\theta_1}{[(\omega - \omega_g)^2 + \Gamma^2]^{1/4}} - \frac{\cos\theta_2}{[(\omega - \omega_0 - \omega_g)^2 + \Gamma^2]^{1/4}} \right] \quad (4)$$

for all values of ω where $\theta_1 = \frac{1}{2}\tan^{-1}[\Gamma/(\omega - \omega_g)]$ and

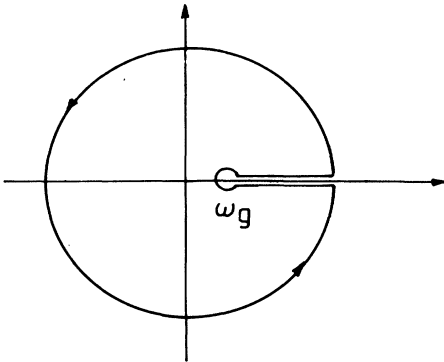


FIG. 1. Contour used to evaluate the integral in Eq. (3).

$\theta_2 = \frac{1}{2}\tan^{-1}[\Gamma/(\omega - \omega_0 - \omega_g)]$. A constant background density of states will only contribute a constant term to Raman amplitude. Similarly, RS amplitude at the M_3 edge can be calculated by considering the negative effective mass

$$\omega_k = \omega_g - hk_z^2/2m \quad (5)$$

so that for the M_3 edge one gets

$$A(\omega) \sim \int_0^{\omega_g} \frac{(\omega_g - \omega_k)^{-1/2} d\omega_k}{(\omega_k - \omega + i\Gamma)(\omega_k - \omega + \omega_0 + i\Gamma)}. \quad (6)$$

We find using the contour in Fig. 2 that the Raman amplitude at the M_3 edge is

$$A(\omega) \sim \frac{1}{\omega_0} \left[\frac{\sin\theta_1}{[(\omega_g - \omega)^2 + \Gamma^2]^{1/4}} - \frac{\sin\theta_2}{[(\omega_g + \omega_0 - \omega)^2 + \Gamma^2]^{1/4}} \right] + \frac{i}{\omega_0} \left[\frac{\cos\theta_1}{[(\omega_g - \omega)^2 + \Gamma^2]^{1/4}} - \frac{\cos\theta_2}{[(\omega_g + \omega_0 - \omega)^2 + \Gamma^2]^{1/4}} \right] \quad (7)$$

for all values of ω where $\theta_1 = \frac{1}{2}\tan^{-1}[\Gamma/(\omega - \omega_g)]$ and $\theta_2 = \frac{1}{2}\tan^{-1}[\Gamma/(\omega - \omega_0 - \omega_g)]$.

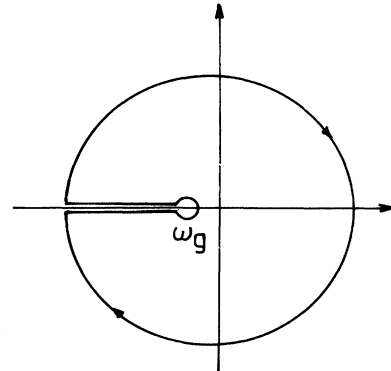


FIG. 2. Contour used to evaluate the integral in Eq. (6).

III. EXCITON EFFECTS: SLATER-KOSTER INTERACTION

So far we have considered free electron-hole ($e-h$) pairs as the intermediate scattering states. A simple model incorporating electron-hole interaction is that due to Slater and Koster where $V(r)=\delta(r)g$, which is zero except when the electron and hole are in the same unit cell. This model has been used to discuss metamorphism of the singularities due to electron-hole interaction by Velicky and Sak²⁰ and Toyozawa *et al.*²¹

The Slater-Koster potential¹¹ in the k representation is given by

$$\langle k|v|k'\rangle = gN^{-1}\delta_{kk'},$$

for all states belonging to a given set of valence and conduction bands. N is the number of unit cells per unit volume and g is the constant which gives the strength of the interaction.

The RS amplitude at the M_0 edge can be written as

$$A(\omega) \sim \int_0^{k_{\max}} \frac{dk_z |\phi^s(0)|^2}{(\omega_k - \omega + i\Gamma)(\omega_k - \omega + \omega_0 + i\Gamma)}, \quad (8)$$

where $\phi^s(0)$ is the envelope function describing the electron-hole from Velicky and Sak;²⁰ we have

$$|\phi^s(0)|^2 = \frac{1}{|1 + gF(\omega)|^2}, \quad (9)$$

where

$$F(\omega) = -N^{-1} \int_{-\infty}^{\infty} \frac{d\omega' N_d(\omega')}{(\omega - \omega' + i\eta)}, \quad (10)$$

$N_d(\omega')$ being the joint density of states.

For $gF(\omega) \ll 1$,

$$\frac{1}{|1 + gF(\omega)|^2} = 1 - 2g \operatorname{Re}F(\omega). \quad (11)$$

Then for $g < 0$ Eq. (8) becomes

$$A(\omega) \sim \frac{1}{\omega_0} \left[\frac{\sin\theta_1}{[(\omega - \omega_g)^2 + \Gamma^2]^{1/4}} - \frac{\sin\theta_2}{[(\omega - \omega_0 - \omega_g)^2 + \Gamma^2]^{1/4}} + \frac{2|g|\pi C\Gamma}{(\omega_g - \omega)^2 + \Gamma^2} - \frac{2|g|\pi C\Gamma}{(\omega_g - \omega + \omega_0)^2 + \Gamma^2} \right] \\ + \frac{i}{\omega_0} \left[\frac{\cos\theta_1}{[(\omega - \omega_g)^2 + \Gamma^2]^{1/4}} - \frac{\cos\theta_2}{[(\omega - \omega_0 - \omega_g)^2 + \Gamma^2]^{1/4}} + \frac{2|g|C(\omega_g - \omega)\pi}{[(\omega_g - \omega)^2 + \Gamma^2]} - \frac{2|g|C(\omega_g - \omega + \omega_0)\pi}{(\omega_g - \omega + \omega_0)^2 + \Gamma^2} \right] \quad (18)$$

for all values of ω where $\theta_1 = \frac{1}{2}\tan^{-1}[\Gamma/(\omega - \omega_g)]$ and $\theta_2 = \frac{1}{2}\tan^{-1}[\Gamma/(\omega - \omega_0 - \omega_g)]$. Similarly one can calculate the Raman amplitude at M_3 point as

$$A(\omega) \sim \frac{1}{\omega_0} \left[\frac{\sin\theta_1}{[(\omega_g - \omega)^2 + \Gamma^2]^{1/4}} - \frac{\sin\theta_2}{[(\omega_g + \omega_0 - \omega)^2 + \Gamma^2]^{1/4}} - \frac{2|g|\pi C\Gamma}{(\omega_g - \omega)^2 + \Gamma^2} + \frac{2|g|\pi C\Gamma}{(\omega_g - \omega + \omega_0)^2 + \Gamma^2} \right] \\ + \frac{i}{\omega_0} \left[\frac{\cos\theta_1}{[(\omega_g - \omega)^2 + \Gamma^2]^{1/4}} - \frac{\cos\theta_2}{[(\omega_g + \omega_0 - \omega)^2 + \Gamma^2]^{1/4}} - \frac{2|g|\pi C(\omega_g - \omega)}{(\omega_g - \omega)^2 + \Gamma^2} + \frac{2|g|C(\omega_g - \omega + \omega_0)\pi}{(\omega_g - \omega + \omega_0)^2 + \Gamma^2} \right] \quad (19)$$

$$A(\omega) \sim \int_0^{\infty} \frac{dk_z [1 + 2|g|\operatorname{Re}F(\omega_k)]}{(\omega_k - \omega + i\Gamma)(\omega_k - \omega + \omega_0 + i\Gamma)}, \quad (12)$$

where the real part of $F(\omega)$ is the Hilbert transform of $N_d(\omega)$:

$$\operatorname{Re}F(\omega) = N^{-1} \mathcal{P} \int_{-\infty}^{\infty} \frac{d\omega' N_d(\omega')}{(\omega' - \omega)}. \quad (13)$$

The RS amplitude at the M_0 point can be calculated by rewriting Eq. (12) with the help of Eq. (2):

$$A(\omega) \sim \int_0^{\infty} \frac{d\omega_k (\omega_k - \omega_g)^{-1/2} [1 + 2|g|\operatorname{Re}F(\omega_k)]}{(\omega_k - \omega + i\Gamma)(\omega_k - \omega + \omega_0 + i\Gamma)}. \quad (14)$$

A simple integration of Eq. (13) gives $\operatorname{Re}F(\omega)$ at the M_0 point:

$$\operatorname{Re}F(\omega) \sim \begin{cases} -\pi(\omega_g - \omega)^{-1/2} & \text{if } \omega < \omega_g \\ 0 & \text{if } \omega > \omega_g \end{cases} \quad (15)$$

and for the M_3 point one gets

$$\operatorname{Re}F(\omega) \sim \begin{cases} \pi(\omega - \omega_g)^{-1/2} & \text{if } \omega > \omega_g \\ 0 & \text{if } \omega < \omega_g \end{cases}. \quad (16)$$

Combining Eqs. (14) and (15) one gets

$$A(\omega) \sim \int_{\omega_g}^{\infty} \frac{(\omega_k - \omega_g)^{-1/2} d\omega_k}{(\omega_k - \omega + i\Gamma)(\omega_k - \omega + \omega_0 + i\Gamma)} \\ - \frac{2|g|\pi}{\omega_0} \int_0^{\omega_g} \frac{(\omega_k - \omega_g)^{-1/2} (\omega_g - \omega_k)^{-1/2}}{(\omega_k - \omega + i\Gamma)(\omega_k - \omega + \omega_0 + i\Gamma)}. \quad (17)$$

The second term of Eq. (17) will be a slowly varying function of ω near ω_g which we call C . The first integral of Eq. (17) will be solved with the help of suitable contours shown in Figs. 1 and 2. Then at the M_0 point, we obtain

for all values of ω where $\theta_1 = \frac{1}{2} \tan^{-1}[\Gamma/(\omega - \omega_g)]$ and $\theta_2 = \frac{1}{2} \tan^{-1}[\Gamma/(\omega - \omega_0 - \omega_g)]$.

For small damping the resonance curve predicts double resonance behavior at ω_g and $\omega_g + \omega_0$ corresponding to incoming and outgoing photons for both interacting and noninteracting e - h pairs. However, for large damping $\Gamma \sim \omega_0$, a single peak falling roughly halfway between the two resonances is expected. The phenomenological damping parameter Γ , which we assume to be a constant, removes the artificial divergence for negligible damping.

IV. EXPERIMENTAL PROCEDURE

Single-crystal platelets of ZrS_3 were prepared by chemical vapor transport using sulfur excess as the transporting agent. Thick single crystals about $4 \times 0.5 \times 0.5 \text{ mm}^3$ were obtained with 50 Torr of S_2 in temperature conditions 620 – 750°C in an evacuated sealed silica tube when the source temperature is 850°C . The single crystals were characterized by microprobe analysis, x-ray diffraction technique, and optical absorption of the $[\text{Zr}]/[\text{S}]$ ratio samples. X-ray patterns show that the structure is a monoclinic one with crystallographic parameters as $a = 5.06$, $b = 3.60$, $c = 8.95 \text{ \AA}$, and $B = 98.5^\circ$ determined from ground single crystals. These results agree with those obtained by Schairer and Shafer.²² The absorption measurements show that the fundamental optical gap energies are about 2.8 eV at room temperature.

Resonance Raman scattering experiments were done in the backscattering geometry. The scattered light was scanned with a double monochromator and the signal was detected by photon counting electronics.

Resonance near the direct gap was studied in ZrS_3 by using various argon-ion laser lines and the temperature tuning the gap. The sample was mounted in a closed cycle cryostat and temperature was obtained by conduction cooling and measured with a calibrated gold thermocouple. The incident laser power was kept below 100 mW to avoid sample heating effects. The lifetime broadening of the phonon modes does not vary appreciably with temperature.

The absorption corrected Raman intensities have been normalized to the intensity of the 520-cm^{-1} line of silicon as the resonance effect of silicon²³ is very well known between 1.8 and 3.7 eV at elevated temperatures.

V. RESULTS AND DISCUSSION

Figure 3 displays the Raman spectra from a quasi-one-dimensional ZrS_3 crystal at various temperatures for the 4880-\AA (2.54-eV) laser line. At room temperature, the Raman spectrum consists of three dominant A_g modes at 150 , 280 , and 320 cm^{-1} and assigned^{5,7} as libration R'_y motion, totally symmetry stretching mode of Zr-S(I) interchain bonds and the ν_s (ZrS_2^{2-}) vibration, respectively. In addition, there are weak bands in the frequency range 200 – 250 cm^{-1} which are B_g modes of rigid sublattice. Polarization effects were not discriminated in our experiments, thus averaging over the anisotropies.

At lower temperature, the A_g modes shift to higher frequencies. Further, the direct energy gap transition in

ZrS_3 crystal exhibits negative temperature coefficient and is in resonance with incident photon energy ($\omega_i \sim 2.54 \text{ eV}$) at 180 K . Figure 3(b) shows enhancement of all A_g modes at resonance. The peak at 280 cm^{-1} shows sharper enhancement than the other two peaks at 150 and 320 cm^{-1} . The resonance enhancement of the B_g modes, on the other hand, is rather weak. In fact, the B_g modes are not completely resolved at 180 K and are resolved into structure at 204 and 215 cm^{-1} at 20 K as shown in Fig. 3(c).

Figure 4 shows the resonance Raman spectra of ZrS_3 crystal near the direct energy gap transition at ω_g (180 K) $\sim 2.54 \text{ eV}$ using different laser wavelengths. The oscillator strength of A_g modes at 280 and 320 cm^{-1} increases with decreasing laser wavelength and is maximum for $\lambda_L = 4880 \text{ \AA}$. The low-frequency mode at 150 cm^{-1} shows anomalous behavior, the mode becomes weak for $\lambda_L = 5017 \text{ \AA}$ and gains strength on further lowering the laser wavelength. The B_g modes in the frequency range 200 – 250 cm^{-1} are very weak off resonance but appear

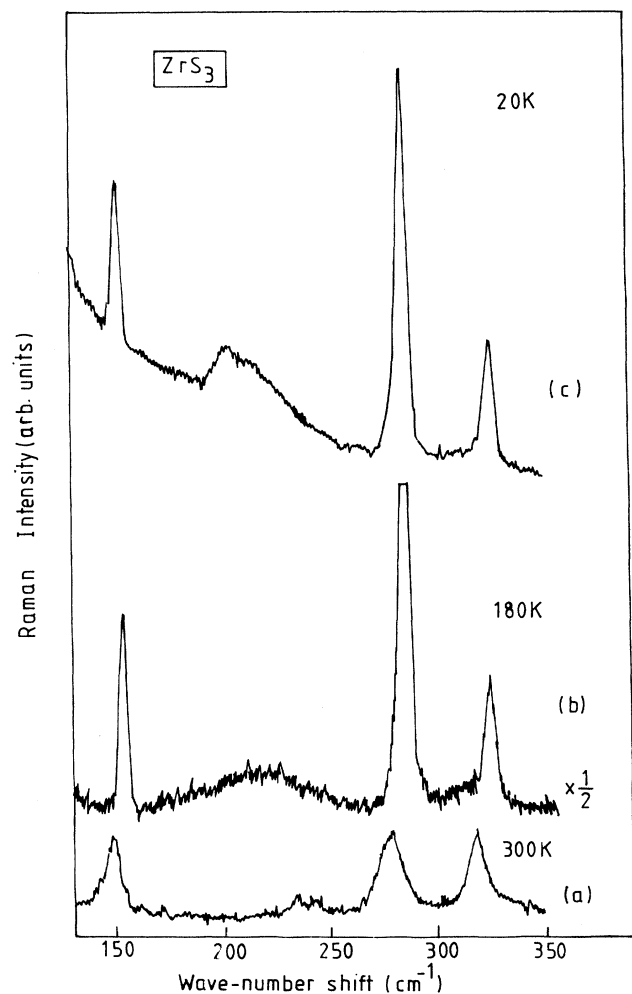


FIG. 3. Unpolarized Raman spectra of ZrS_3 at different temperatures (a) 300 K , (b) 180 K , and (c) 20 K with $\lambda_L = 4880 \text{ \AA}$.

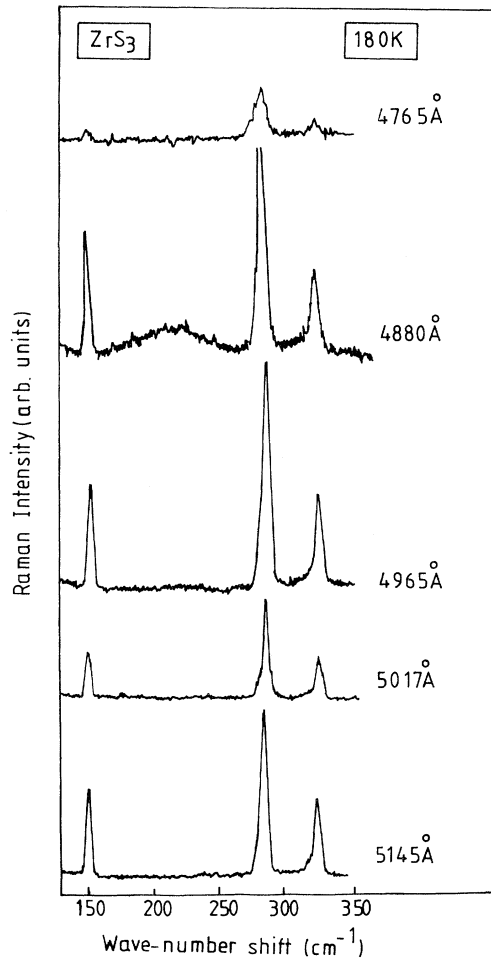


FIG. 4. Unpolarized resonance Raman spectra of ZrS_3 at 180 K using different wavelengths of argon-ion laser.

TABLE I. Phonon modes at 180 K in quasi-one-dimensional ZrS_3 crystal.

Band maxima published (Ref. 7)	Our expt.	Symmetry	Assignment
21		B_g	Acoustic rigid chain
85		B_g	Shearing
109		B_g	Shearing
123		A_g	Acoustic rigid chain
143	147	A_g	Acoustic rigid chain
152	156	A_g	Libration R'_y
	220	B_g	2×109
238	234	A_g	$152 + 85$
248	244	B_g	Rigid sublattice
261		B_g	$152 + 109$
280	280	A_g	$\nu_{Zr-S(1)}$ interchain bonds
285	286	A_g	
307	312	B_g	2×156
320	326	A_g	$\nu_s ZrS_2^{2-}$ intrachain bonds

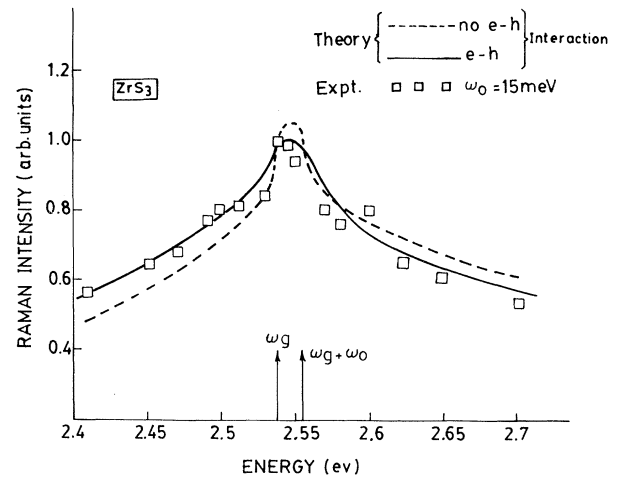


FIG. 5. Resonance curve of ZrS_3 at 180 K for $h\omega_0 = 15$ meV. The solid line shows $e-h$ interaction fit to Eq. (18) taking $h\omega_g = 2.54$ eV, $|g| = 0.1$ eV, $h\Gamma = 30$ meV. Raman intensity is plotted on \log_{10} scale.

near resonance for $\lambda_L = 4880$ Å. These modes appear as a broad band. Table I lists observed phonon modes at 180 K in a quasi-one-dimensional ZrS_3 crystal.

Figures 5, 6, and 7 show the resonances of these A_g modes near the direct-gap transition in quasi-one-dimensional ZrS_3 . The experimental points in Figs. 5–7 were collected in the temperature range between 300 and 150 K and in this range the lifetime broadening of the phonon modes does not vary appreciably with temperature, so that the damping factor is a constant in this temperature range. The theoretical Raman intensities are calculated for each A_g phonon using Eqs. (18), taking $g = 0.1$ eV and $\Gamma = 30$ meV as adjustable parameters. The

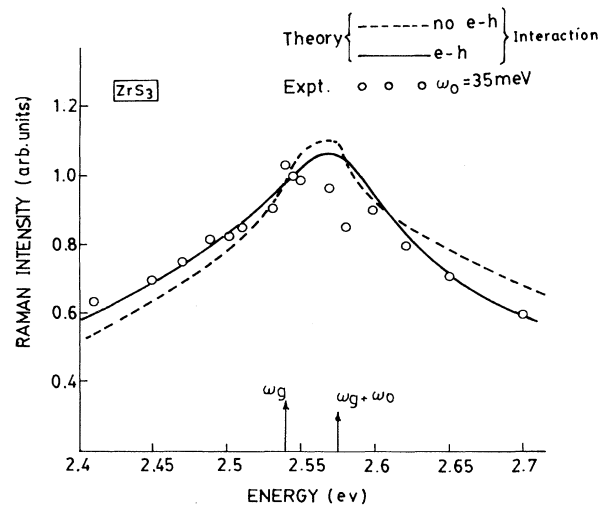


FIG. 6. Resonance curve of ZrS_3 for $h\omega_0 = 35$ meV. Other parameters are the same as in Fig. 5.

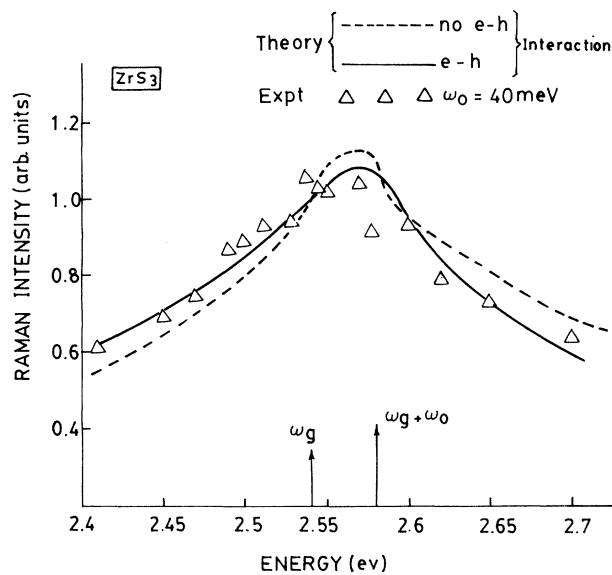


FIG. 7. Resonance curve of ZrS_3 for $h\omega_0=40$ meV. Other parameters are the same as in Fig. 5.

values of $\Gamma=30$ meV and $g=0.1$ eV are consistent with the values quoted by other authors.^{18,19} The value of constant C has been chosen arbitrarily. The experimental results are in good agreement with theory.

Our experimental results show a one-singularity resonant structure in ZrS_3 is due to large damping of intermediate scattering states. This is consistent with previously reported¹⁸ values of Γ in this crystal. In II-VI compounds,²⁴ the absence of outgoing resonance to $h\omega_L=h\omega_g+h\omega_0$ can be explained by a three-dimensional (3D) theory which assumes a strong Coulomb interaction between electrons and holes in the intermediate state. We would normally expect singular structure at $\omega=\omega_g$ and $\omega=\omega_g+\omega_0$ corresponding to resonance of the incoming and outgoing photons with intermediate scattering states. For small damping, a two-peak

structure is expected. On increasing Γ towards ω_0 , the two resonances begin to overlap until for $\Gamma\sim\omega_0$. Only a single resonance is seen between $\omega=\omega_g$ and $\omega=\omega_g+\omega_0$. We have calculated the Raman intensity in a quasi-1D system using Eqs. (4) and (18) in our theory, which exhibits a single resonance structure falling roughly in between the incoming and outgoing resonances for damping such that $\Gamma\sim\omega_0$. This is irrespective of the strength of the electron-hole interaction.

VI. CONCLUSION

We have presented a detailed theory of resonant Raman scattering in a quasi-one-dimensional system near M_0 singularity. A two-peaked resonant structure would be seen for small values of Γ . On increasing Γ one obtains overlapping resonances corresponding to the incoming and outgoing photons. In this case the theory predicts a single-peak structure situated roughly between the incoming and outgoing photon resonances for both free and interacting electron-hole pairs as intermediate scattering states. We conjecture that the one-singularity resonance structure in ZrS_3 is due to large damping of the intermediate scattering states.

The experimental data on a quasi-one-dimensional ZrS_3 crystal near the direct-gap transition are in consonance with our theory which is appropriate to Raman scattering in a one-dimensional crystal near the M_0 singularity. The damping factor is taken as an adjustable parameter in the theory to match the maximum of the theoretical resonance curve to that of experimental curve. For the M_0 singularity at 2.54 eV the results are in good agreement both below and above the transition energy. It is interesting to note that double resonance effects are seen in Raman scattering from some 2D crystals like GaSe,²⁵ but neither in 3D or in 1D materials. The basic reason for the occurrence of either incoming or outgoing resonances or both in Raman scattering from semiconductors is not known. This is an interesting problem which remains unsolved.

¹T. J. Wieting, A. Grisel, F. Levy, and Ph. Schmid, in *Quasi-One-Dimensional Conductors I*, Vol. 95 of Lecture Notes in Physics (Springer-Verlag, Berlin, 1979), p. 354.

²S. Jandl, C. Deville Cavellin, and J. Y. Harbec, *Solid State Commun.* **31**, 351 (1979).

³J. Y. Herbec, C. Deville Cavellin, and J. Jandl, *Phys. Status Solidi* **96**, K117 (1979).

⁴C. Deville Cavellin and S. Jandl, *Phys. Status Solidi B* **33**, 813 (1980).

⁵A. Zwick, M. A. Renucci, and A. Kjekshus, *J. Phys. C* **13**, 5603 (1980).

⁶S. Jandl, M. Banville, and J. Y. Harbec, *Phys. Rev. B* **22**, 5697 (1980).

⁷C. Sourisseau and Y. Mathey, *Chem. Phys. Lett.* **74**, 128 (1980).

⁸S. H. Chen, *Phys. Rev.* **163**, 532 (1967).

⁹A. Grisel, F. Levy, and T. J. Wieting, *Physica* **99B**, 365 (1980).

¹⁰T. J. Wieting, A. Grisel, and F. Levy, *Physica* **105B**, 366 (1981).

¹¹A. Zwick, M. A. Renucci, R. Carles, N. Saint-Cricq, and J. B. Renucci, *Physica* **105B**, 361 (1981).

¹²S. Furuseth, L. Brattas, and A. Kjekshus, *Acta Chem. Scand.* **29**, 623 (1975).

¹³A. Meershaut and J. Rouxell, *J. Less-Common Met.* **39**, 197 (1975).

¹⁴E. Bjerkelund, J. H. Fermor, and A. Kjekshus, *Acta Chem. Scand.* **20**, 1836 (1966).

¹⁵N. P. Ong and P. Monceau, *Phys. Rev. B* **16**, 3433 (1977).

¹⁶D. W. Galliardt, W. R. Nieveen, and R. D. Kirby, *Solid State Commun.* **34**, 37 (1980).

¹⁷S. Kurita, J. L. Stalhli, M. Guzzi, and F. Levy, *Physica* **105B**, 169 (1981).

¹⁸S. Kurita, Y. Okada, and M. Tanaka, *Helv. Phys. Acta* **58**,

- 321 (1985).
- ¹⁹K. P. Jain and Gyatri Choudhury, *Phys. Rev. B* **8**, 676 (1973).
- ²⁰B. Velicky and J. Sak, *Phys. Status Solidi* **16**, 147 (1966).
- ²¹Y. Toyozawa *et al.*, *J. Phys. Soc. Jpn.* **22**, 1337 (1967).
- ²²W. Schairer and M. W. Shafer, *Phys. Status Solidi* **17a**, 181 (1973).
- ²³A. Compagn and H. J. Trodhl, *Phys. Rev. B* **29**, 793 (1984).
- ²⁴F. Bechstedt and D. Haus, *Phys. Status Solidi B* **88**, 163 (1978).
- ²⁵J. Reydellet, M. Balkanski, and J. M. Besson, *J. Phys. (Paris) Lett.* **37**, L219 (1976).